Resonance enhancement of magnetic Faraday rotation

A. Figotin and I. Vitebskiy

Abstract. Magnetic Faraday rotation is widely used in optics. In natural transparent materials, this effect is very weak. One way to enhance it is to incorporate the magnetic material into a periodic layered structure displaying a high-Q resonance. One problem with such magneto-optical resonators is that a significant enhancement of Faraday rotation is inevitably accompanied by strong ellipticity of the transmitted light. More importantly, along with the Faraday rotation, the resonator also enhances linear birefringence and absorption associated with the magnetic material. The latter side effect can put severe limitations on the device performance. From this perspective, we carry out a comparative analysis of optical microcavity and a slow wave resonator. We show that slow wave resonator has a fundamental advantage when it comes to Faraday rotation enhancement in lossy magnetic materials.

1. Introduction

Nonreciprocal effects play a crucial role in microwave technology and optics. They are absolutely essential in numerous devices such as isolators, circulators, phase shifters, etc. Nonreciprocal effects in optics and MW occur in magnetically ordered materials or in the presence of magnetic field [1, 2]. A well-known example is magnetic Faraday rotation related to nonreciprocal circular birefringence. At optical frequencies, all nonreciprocal effects are usually weak, and can be further obscured by absorption, linear birefringence, etc. A way to enhance a weak Faraday rotation is to place the magnetic material in an optical resonator [3, 4, 5, 6, 7, 8, 9, 10]. An intuitive explanation for the resonance enlacement invokes a simple idea that in a high-Q optical resonator filled with magnetic material, each individual photon resides much longer compared to the same piece of magnetic material taken out of the resonator. Since the nonreciprocal circular birefringence is independent of the direction of light propagation, one can assume that the magnitude of Faraday rotation is proportional to the photon residence time in the magnetic material. With certain reservations, the above assumption does provide a hand-waving explanation of the phenomenon of resonance enhancement of weak Faraday rotation. The problem, though, is that the above qualitative picture of the phenomenon does not apply to composite structures in which the size of magnetic components is comparable to or lesser than the electromagnetic wavelength. At the same time, all the existing methods of resonance enhancement of nonreciprocal effects involve some kind of composite dielectric structures, such as periodic layered arrays, in which the magnetic layer thickness is comparable to the electromagnetic wavelength.

In this paper we analyze and compare two qualitatively different approaches to resonance enhancement of magnetic Faraday rotation. The first one is based on a magnetic microcavity sandwiched between a pair of Bragg reflectors, as shown in Fig. 1. The second approach is based on a slow wave resonance in a magnetic photonic crystal, an example of which is shown in Fig. 2. Either approach involves spatially periodic composite structures, usually, periodic layered arrays. In either case, the thickness of magnetic layers producing Faraday rotation has to be comparable to the electromagnetic wavelength. Otherwise, the resonance enhancement becomes inefficient. On the other hand, a linearly polarized electromagnetic wave entering such a magnetic composite structure inevitably acquires ellipticity, which in this case is a manifestation of nonreciprocity [14]. If the resonance Q-factor is high enough, the acquired ellipticity becomes so significant that the very term "Faraday rotation" becomes irrelevant. Indeed, one cannot assign a meaningful rotation angle to a wave with nearly circular polarization. The above circumstance, though, does not diminish the practical importance of the nonreciprocal effect, which now reduces to the conversion of linear polarization of the incident wave to nearly circular polarization of transmitted and/or reflected waves.

The resonance conditions can result in enhancement of the nonreciprocal effect, which is a desirable outcome. On the other hand, the same resonance conditions will also cause enhancement of absorption and linear birefringence in the same magnetic material, which is undesirable. Linear birefringence, if present, can drastically suppress the Faraday rotation, or any other manifestation of nonreciprocal circular birefringence. Even more damaging can be absorption. In uniform magnetic materials, the absorption contributes to the ellipticity of transmitted wave and causes circular dichroism. In low-loss magnetic materials those effects can be insignificant. Under the

resonance condition, though, the role of absorption can change dramatically. Firstly, the enhanced absorption reduces the intensity of light transmitted through the optical resonator. Secondly, even moderate absorption can lower the Q-factor of the resonance by several orders of magnitude and, thereby, significantly compromise its performance as Faraday rotation enhancer. The role of absorption essentially depends on whether it is a microcavity or a photonic slow wave resonator. It turns out that the resonance cavity shown in Fig. 1 is particularly vulnerable to absorption. This and related questions are also addressed in this paper.

2. Notations, definitions, and physical assumptions

2.1. Transverse electromagnetic waves in stratified media

Our analysis is based on the time-harmonic Maxwell equations

$$\nabla \times \vec{E}\left(\vec{r}\right) = i\frac{\omega}{c}\hat{\mu}\left(\vec{r}\right)\vec{H}\left(\vec{r}\right),\ \nabla \times \vec{H}\left(\vec{r}\right) = -i\frac{\omega}{c}\hat{\varepsilon}\left(\vec{r}\right)\vec{E}\left(\vec{r}\right), \tag{1}$$

where the second rank tensors $\hat{\varepsilon}\left(\vec{r}\right)$ and $\hat{\mu}\left(\vec{r}\right)$ are coordinate dependent. In a stratified medium

$$\hat{\varepsilon}\left(\vec{r}\right) = \hat{\varepsilon}\left(z\right), \hat{\mu}\left(\vec{r}\right) = \hat{\mu}\left(z\right),$$

where the Cartesian coordinate z is normal to the layers. We also assume that the dielectric permittivity and magnetic permeability tensors in each layer has the following form

$$\hat{\varepsilon} = \begin{bmatrix} \varepsilon_{xx} & \varepsilon_{xy} & 0 \\ \varepsilon_{yx} & \varepsilon_{yy} & 0 \\ 0 & 0 & \varepsilon_{zz} \end{bmatrix},\ \ \hat{\mu} = \begin{bmatrix} \mu_{xx} & \mu_{xy} & 0 \\ \mu_{yx} & \mu_{yy} & 0 \\ 0 & 0 & \mu_{zz} \end{bmatrix}, \tag{2}$$

in which case the layered structure support transverse electromagnetic waves with

$$\vec{E}\left(\vec{r}\right) = \vec{E}\left(z\right) \perp z,\ \vec{H}\left(\vec{r}\right) = \vec{H}\left(z\right) \perp z, \tag{3}$$

propagating along the z direction. The Maxwell equations (1) in this case reduce to the following system of four ordinary differential equations

$$\frac{\partial}{\partial z}\Psi\left(z\right) = i\frac{\omega}{c}M\left(z\right)\Psi\left(z\right), \tag{4}$$

where

$$\Psi\left(z\right) = \begin{bmatrix} E_x\left(z\right) \\ E_y\left(z\right) \\ H_x\left(z\right) \\ H_y\left(z\right) \end{bmatrix}, \tag{5}$$

and

$$M\left(z\right) = \begin{bmatrix} 0 & 0 & \mu_{xy}^{*} & \mu_{yy} \\ 0 & 0 & -\mu_{xx} & -\mu_{xy} \\ -\varepsilon_{xy}^{*} & -\varepsilon_{yy} & 0 & 0 \\ \varepsilon_{xx} & \varepsilon_{xy} & 0 & 0 \end{bmatrix}. \tag{6}$$

The 4×4 matrix $M\left(z\right)$ is referred to as the (reduced) Maxwell operator.

Solutions for the reduced time-harmonic Maxwell equation (4) can be presented in the following form

$$\Psi(z) = T(z, z_0)\,\Psi(z_0), \tag{7}$$

where the 4×4 matrix $T(z, z_0)$ is the *transfer matrix*. The transfer matrix (7) uniquely relates the values of electromagnetic field (5) at any two points z and z_0 of the stratified medium.

In a uniform medium, the Maxwell operator M in (6) is independent of z. In this case, the transfer matrix $T(z, z_0)$ can be explicitly expressed in terms of the respective Maxwell operator M

$$T(z, z_0) = \exp\left[i\frac{\omega}{c}(z - z_0)\,M\right]. \tag{8}$$

In particular, the transfer matrix of an individual uniform layer m is

$$T_m = \exp\left(i\frac{\omega}{c}z_m M_m\right), \tag{9}$$

where z_m is the thickness of the m-th layer.

The transfer matrix T_S of an arbitrary stack of layers is a sequential product of the transfer matrices T_m of the constituent layers

$$T_S = \prod_m T_m. \tag{10}$$

In the following subsection we specify the form of the material tensors (2), which determine the transfer matrices of the individual layers and the entire periodic structure. In this paper, we use the same notations as in our previous publication [12, 13, 14] related to magnetic layered structures.

2.2. Permittivity and permeability tensors of the layers

We assume that the permittivity and permeability tensors of individual layers have the following form

$$\hat{\varepsilon} = \begin{bmatrix} \varepsilon+\delta & i\alpha & 0 \\ -i\alpha & \varepsilon-\delta & 0 \\ 0 & 0 & \varepsilon_{zz} \end{bmatrix}, \quad \hat{\mu} = 1, \tag{11}$$

where α is responsible for nonreciprocal circular birefringence and δ describes linear birefringence. In a lossless medium, the physical quantities ε, α, and δ are real. If the direction of magnetization is changed for the opposite, the parameters α also changes its sign and so will the sense of Faraday rotation [1, 2]. The absorption, is accounted for by allowing ε, α, and δ to be complex.

Substitution of (11) into (6) yields the following expression for the Maxwell operator

$$M = \begin{bmatrix} 0 & 0 & 0 & 1 \\ 0 & 0 & -1 & 0 \\ i\alpha & -\varepsilon+\delta & 0 & 0 \\ \varepsilon+\delta & i\alpha & 0 & 0 \end{bmatrix}. \tag{12}$$

The respective four eigenvectors are

$$\left\{\begin{array}{c}1\\-ir_1\\in_1r_1\\n_1\end{array}\right\}\leftrightarrow n_1,\ \left\{\begin{array}{c}1\\-ir_1\\-in_1r_1\\-n_1\end{array}\right\}\leftrightarrow -n_1,\ \left\{\begin{array}{c}-ir_2\\1\\-n_2\\-in_2r_2\end{array}\right\}\leftrightarrow n_2,\ \left\{\begin{array}{c}-ir_2\\1\\n_2\\in_2r_2\end{array}\right\}\leftrightarrow -n_2. \tag{13}$$

where

$$n_1=\sqrt{\varepsilon+\sqrt{\delta^2+\alpha^2}},\ \ n_2=\sqrt{\varepsilon-\sqrt{\delta^2+\alpha^2}}, \tag{14}$$

$$r_1=\frac{\alpha}{\sqrt{\delta^2+\alpha^2}+\delta},\ r_2=\frac{\sqrt{\delta^2+\alpha^2}-\delta}{\alpha}, \tag{15}$$

Compared to [6], we use slightly different notations.

The explicit expression for the transfer matrix $\hat{T}(A)$ of a single uniform layer of thickness A is

$$\hat{T}(A)=\hat{W}\left(A\right)\hat{W}^{-1}(0), \tag{16}$$

where

$$\hat{W}\left(A\right)=\left[\begin{array}{cccc}e^{i\phi_1} & e^{-i\phi_1} & -ir_2e^{i\phi_2} & -ir_2e^{-i\phi_2}\\ -ir_1e^{i\phi_1} & -ir_1e^{-i\phi_1} & e^{i\phi_2} & e^{-i\phi_2}\\ ir_1n_1e^{i\phi_1} & -ir_1n_1e^{-i\phi_1} & -n_2e^{i\phi_2} & n_2e^{-i\phi_2}\\ n_1e^{i\phi_1} & -n_1e^{-i\phi_1} & -ir_2n_2e^{i\phi_2} & ir_2n_2e^{-i\phi_2}\end{array}\right], \tag{17}$$

and

$$\phi_1=\frac{\omega}{c}An_1,\ \ \phi_2=\frac{\omega}{c}An_2.$$

The eigenvectors (13) correspond to elliptically polarized states. There are two important particular cases corresponding to linearly and circularly polarized eigenmodes, respectively.

2.2.1. Non-magnetic medium with linear birefringence In the case of a non-magnetic medium

$$\alpha=0,\ r_1=0,\ r_2=0. \tag{18}$$

The respective eigenmodes are linearly polarized

$$\left\{\begin{array}{c}1\\0\\0\\n_1\end{array}\right\}\leftrightarrow n_1,\ \left\{\begin{array}{c}1\\0\\0\\-n_1\end{array}\right\}\leftrightarrow -n_1,\ \left\{\begin{array}{c}0\\1\\-n_2\\0\end{array}\right\}\leftrightarrow n_2,\ \left\{\begin{array}{c}0\\1\\n_2\\0\end{array}\right\}\leftrightarrow -n_2. \tag{19}$$

where

$$n_1=\sqrt{\varepsilon+\delta},\ \ n_2=\sqrt{\varepsilon-\delta}.$$

2.2.2. Magnetic medium with circular birefringence Another important limiting case corresponds to a uniaxial magnetic medium with

$$\delta=0,\ r_1=1,\ r_2=1. \tag{20}$$

The respective eigenmodes are circularly polarized

$$\left\{\begin{array}{c}1\\-i\\in_1\\n_1\end{array}\right\}\leftrightarrow n_1,\ \left\{\begin{array}{c}1\\-i\\-in_1\\-n_1\end{array}\right\}\leftrightarrow -n_1,\ \left\{\begin{array}{c}-i\\1\\-n_2\\-in_2\end{array}\right\}\leftrightarrow n_2,\ \left\{\begin{array}{c}-i\\1\\n_2\\in_2\end{array}\right\}\leftrightarrow -n_2. \quad (21)$$

where

$$n_1=\sqrt{\varepsilon+\alpha},\quad n_2=\sqrt{\varepsilon-\alpha}.$$

2.3. Numerical values of material tensors

Our objectives include two distinct problems associated with Faraday rotation enhancement.

One problem can be caused by the presence of linear birefringence described by the parameter δ in (11). Linear birefringence δ competes with circular birefringence α. At optical frequencies, the former can easily prevail and virtually annihilate any manifestations of nonreciprocal circular birefringence. If linear birefringence occurs in magnetic F layers in Fig. 2, it can be offset by linear birefringence in the alternating dielectric A layers. Similarly, in the case of a magnetic resonance cavity in Fig. 1, the destructive effect of the linear birefringence in the magnetic D layer can be offset by linear birefringence in layers constituting the Bragg reflectors. In either case, the cancellation of linear birefringence of the magnetic layers only takes place at one particular frequency. Therefore, the layered structure should be designed so that this particular frequency coincides with the operational resonance frequency of the composite structure. The detailed discussion on the effect of linear birefringence and ways to deal with it will be presented elsewhere.

In the rest of the paper we will focus on the problem associated with absorption. This problem is unrelated to the presence or absence of linear birefringence and, therefore, can be handled separately. For this reason, in our numerical simulation we can set $\delta=0$ and use the following expressions for the dielectric permittivity tenors of the magnetic F-layers and dielectric A-layers in Fig. 2

$$\hat{\varepsilon}_F=\left[\begin{array}{ccc}\varepsilon_F+i\gamma & i\alpha & 0\\ -i\alpha & \varepsilon_F+i\gamma & 0\\ 0 & 0 & \varepsilon_3\end{array}\right], \quad (22)$$

$$\hat{\varepsilon}_A=\left[\begin{array}{ccc}\varepsilon_A & 0 & 0\\ 0 & \varepsilon_A & 0\\ 0 & 0 & \varepsilon_A\end{array}\right], \quad (23)$$

where ε_F, ε_A, and γ are real. Parameter γ describes absorption of the magnetic material.

In the case of photonic cavity in Fig. 1 we use similar material parameters. The permittivity tensor of the magnetic D-layer is the same as that of the magnetic F-layers in Fig. 2

$$\hat{\varepsilon}_D=\hat{\varepsilon}_F \quad (24)$$

$\hat{\varepsilon}_F$ is defined in (22). The permittivity tensors of the alternating dielectric layers A and B constituting the Bragg reflectors in Fig. 1 are chosen as follows

$$\hat{\varepsilon}_B=\left[\begin{array}{ccc}\varepsilon_B & o & 0\\ 0 & \varepsilon_B & 0\\ 0 & 0 & \varepsilon_B\end{array}\right],\ \hat{\varepsilon}_C=\left[\begin{array}{ccc}\varepsilon_C & 0 & 0\\ 0 & \varepsilon_C & 0\\ 0 & 0 & \varepsilon_C\end{array}\right]. \quad (25)$$

In either case, only the magnetic layers F or D are responsible for absorption, which is a realistic assumption.

In the case of periodic stack in Fig. 2 we use the following numerical values of the diagonal components of the permittivity tensors

$$\varepsilon_F = 5.37, \quad \varepsilon_A = 2.1. \tag{26}$$

Similar values are used in the case of photonic microcavity in Fig. 1

$$\varepsilon_D = \varepsilon_C = 5.37, \quad \varepsilon_B = 2.1.$$

The numerical values of the gyrotropic parameter α, as well as the absorption coefficient γ of the magnetic layers F and D, remain variable. We also tried different layer thicknesses d_A, d_F, d_B, d_C, and d_D. But in this paper we only include the results corresponding to the following numerical values

$$d_A = d_C = 0.8L, \; d_F = d_C = 0.2L, \; d_D = 0.4L, \tag{27}$$

where L is the length of a unit cell of the periodic array

$$L = d_F + d_A = d_B + d_C.$$

The thickness d_D of the defect layer in Fig. 1 is chosen so that the frequency of the defect mode falls in the middle of the lowest photonic band gap of Bragg reflectors.

2.4. Scattering problem for magnetic layered structure

In all cases, the incident wave Ψ_I propagates along the z direction normal to the layers. Unless otherwise explicitly stated, the incident wave polarization is linear with $\vec{E}_I \parallel x$. Due to the nonreciprocal circular birefringence of the magnetic material, the transmitted and reflected waves Ψ_P and Ψ_R will be elliptically polarized with the ellipse axes being at an angle with the x direction.

The transmitted and reflected waves, as well the electromagnetic field distribution inside the layered structure, are found using the transfer matrix approach. Let us assume that the left-hand and the right-hand boundaries of a layered array are located at $z = 0$ and $a = d$, respectively. According to (7) and (10), the incident, transmitted, and reflected waves are related as follows

$$\Psi_P(d) = T_S \left(\Psi_I(0) + \Psi_R(0) \right). \tag{28}$$

Knowing the incident wave Ψ_I and the transfer matrix T_S of the entire layered structure and assuming, we can solve the system (28) of four linear equations and, thereby, find the reflected and transmitted waves. Similarly, using the relation (7), we can also find the field distribution inside the layered structure.

The transmission and reflection coefficients of the slab (either uniform, or layered) are defined as follows

$$t = \frac{S_P}{S_I}, \; r = -\frac{S_R}{S_I}, \tag{29}$$

where S_I, S_P, and S_R are the Poynting vectors of the incident, transmitted, and reflected waves, respectively. The slab absorption is

$$a = 1 - t - r. \tag{30}$$

If the incident wave polarization is linear, the coefficients t, r, and a are independent of the orientation of vector $\vec{E}_I$ in the $x-y$ plane, because for now, we neglect the linear birefringence δ. Due to nonreciprocal circular birefringence, the polarization of the transmitted and reflected waves will always be elliptic.

By contrast, if the incident wave polarization is circular, the coefficients t, r, and a depend on the sense of circular polarization. The polarization of the transmitted and reflected waves in this case will be circular with the same sense of rotation as that of the incident wave.

The effect of nonreciprocal circular birefringence on transmitted wave can be quantified by the following expression

$$\Delta\Psi_P = \frac{1}{2}\left[(\Psi_P)_\alpha - (\Psi_P)_{-\alpha}\right] \tag{31}$$

where $(\Psi_P)_\alpha$ and $(\Psi_P)_{-\alpha}$ respectively correspond to the wave transmitted through the original periodic structure and through the same structure but with the opposite sign of circular birefringence parameter α. If the incident wave polarization is linear with $\vec{E}_I \parallel x$, the vector-column (31) has the following simple structure

$$\Delta\Psi_P = \left(\vec{E}_P\right)_y \begin{bmatrix} 0 \\ 1 \\ 1 \\ 0 \end{bmatrix},$$

implying that the y component $\left(\vec{E}_P\right)_y$ of the transmitted wave has "purely" nonreciprocal origin and, therefore, can used to characterize the magnitude of nonreciprocal circular birefringence on transmitted wave. Indeed, in the absence of magnetism, the parameter α in (11), (22), and 24) vanishes and the transmitted wave is linearly polarized with $\vec{E}_P \parallel x$. The above statement follows directly from symmetry consideration and remains valid even in the presence of linear birefringence δ in (11). Further in this paper will use the ratio

$$\rho = \frac{(E_P)_y}{(E_I)_x}, \quad \text{where} \quad |\rho| < 1. \tag{32}$$

to characterize the effect circular birefringence on transmitted wave.

Generally, the transmitted wave polarization in the situation in Figs. 2 and 1 is elliptical, rather than linear. Therefore, the quantity ρ in (32) is not literally the sine of the Faraday rotation angle. Let us elaborate on this point. The electromagnetic eigenmodes of the layered structures in Figs. 2 and 1 with permittivity tensors given in (22) through (25) are all circularly polarized. This implies that if the polarization of the incident wave is circular, the transmitted and reflected waves will also be circularly polarized. On the other hand, due to the nonreciprocal (magnetic) effects, the transmission/reflection coefficients for the right-hand circular polarization are different from those for the left-hand circular polarization. This is true regardless of the presence or absence of absorption. Consider now a linearly polarized incident wave. It can be viewed as a superposition of two circularly polarized waves with equal amplitudes. Since the transmission/reflection coefficients for the right-hand and left-hand circular polarizations are different, the transmitted and reflected waves will be elliptically polarized. Such an ellipticity develops both in the case of a uniform slab

and in the case of a layered stack, periodic or aperiodic, with or without absorption. Note, though, that at optical frequencies, the dominant contribution to ellipticity of the wave transmitted through a uniform slab is usually determined by absorption, which is largely responsible for circular dichroism. Without absorption, the ellipticity of the wave transmitted through a uniform magnetic slab would be negligible. This might not be the case for the layered structures in Figs. 2 and 1 at frequencies of the respective transmission resonances. In these cases, the ellipticity of transmitted and reflected waves can be significant even in the absence of absorption. Moreover, if the Q-factor of the respective resonance is high enough, the transmitted wave polarization becomes very close to circular and, therefore, cannot be assigned any meaningful angle of rotation. The numerical examples of the next section illustrate the above statements.

To avoid confusion, note that a linear polarized wave propagating in a uniform, lossless, unbounded, magnetic medium (22) will not develop any ellipticity. Instead, it will display a pure Faraday rotation. But the slab boundaries and the layer interfaces will produce some ellipticity even in the case of lossless magnetic material. The absorption provides an additional contribution to the ellipticity of transmitted and reflected waves. The latter contribution is referred to as circular dichroism.

For simplicity, in further consideration we will often refer to the quantity ρ in (32) as the amount of (nonreciprocal) Faraday rotation, although, due to the ellipticity, it is not exactly the sine of the Faraday rotation angle.

In all plots, the frequency ω and the Bloch wave number k are expressed in dimensionless units of cL^{-1} and L^{-1}, respectively. In our computations we use a transfer matrix approach identical to that described in Ref. [12, 13].

3. Resonance enhancement of circular birefringence

3.1. Cavity resonance: Lossless case

Let us start with the resonance enhancement based on microcavity. The magnetic layer D in Fig. 1 is sandwiched between two identical periodic stacks playing the role of distributed Bragg reflectors. The D-layer is also referred to as a defect layer, because without it, the layered structure in Fig. 1 would be perfectly periodic. The thickness of the defect layer is chosen so that the microcavity develops a single resonance mode with the frequency lying in the middle of the lowest photonic band gap of the adjacent periodic stacks. This resonance mode is nearly localized in the vicinity of the magnetic D-layer.

A typical transmission spectrum of such a layered structure in the absence of absorption is shown in Fig. 3. The stack transmission develops a sharp peak at the defect mode frequency. The respective transmission resonance is accompanied by a dramatic increase in field amplitude in the vicinity of the magnetic D-layer. The large field amplitude implies the enhancement of magnetic Faraday rotation produced by the D-layer, as clearly seen in Fig. 4.

If the Q-factor of the microcavity exceeds certain value and/or if the circular birefringence of the magnetic material of the D-layer is strong enough, the resonance frequency of the defect mode splits into two, as shown in Fig. 4(c) and (d). Each of the two resonances is associated with left or right circular polarization. The transmitted light will also display nearly perfect circular polarization with the opposite sense of rotation for the twin resonances. Formally, the above nonreciprocal effect cannot be

classified as Faraday rotation, but it does not diminish its practical value.

3.2. Slow wave resonance: Lossless case

The second approach to Faraday rotation enhancement is based on the transmission band edge resonance in periodic stacks of magnetic layers alternating with some other dielectric layers, as shown in Fig. 2. A typical transmission spectrum of such a layered structure is shown in Fig. 7. The sharp peaks in transmission bands correspond to transmission band edge resonances, also known as Fabry-Perot resonances. The resonance frequencies are located close to a photonic band edge, where the group velocity of the respective Bloch eigenmodes is very low. This is why the transmission band edge resonances are referred to as slow wave resonances. All resonance frequencies are located in transmission bands – not in photonic band gaps, as in the case of a localized defect mode. The resonance field distribution inside the periodic stack is close to a standing wave composed of a pair of Bloch modes with equal and opposite group velocities and nearly equal large amplitudes

$$\Psi_T(z) = \Psi_k(z) + \Psi_{-k}(z), \tag{33}$$

The left-hand and right-hand photonic crystal boundaries coincide with the standing wave nodes, where the forward and backward Bloch components interfere destructively to meet the boundary conditions. The most powerful slow wave resonance corresponds to the transmission peak closest to the respective photonic band edge, where the wave group velocity is lowest. At resonance, the energy density distribution inside the periodic structure is typical of a standing wave

$$W(z) \propto W_I N^2 \sin^2\left(\frac{\pi}{NL} z\right), \tag{34}$$

where W_I is the intensity of the incident light, N is the total number of unit cells (double layers) in the periodic stack in Fig. 2.

Similarly to the case of magnetic cavity resonance, the large field amplitude implies the enhancement of magnetic Faraday rotation produced by magnetic F-layers, as demonstrated in Fig. 9. Again, if the Q-factor of the slow wave resonance exceeds certain value and/or if the circular birefringence α of the magnetic material of the F-layers is strong enough, each resonance frequency splits into two, as shown in Fig. 10. Each of the two twin resonances is associated with left or right circular polarization. To demonstrate it, let us compare the transmission dispersion in Fig. 10, where the incident light polarization is linear, to the transmission dispersion in Figs. 11 and 12, where the incident wave is circularly polarized. One can see that the case in Fig. 10 of linearly polarized incident light reduces to a superposition of the cases in Figs. 11 and 12 of two circularly polarized incident waves with opposite sense of rotation.

3.3. The role of absorption

In the absence of absorption, the practical difference between cavity resonance and slow wave resonance is not that obvious. But if the magnetic material displays an appreciable absorption, the difference between the two resonators becomes huge. The physical reason for this is as follows.

In the case of a slow wave resonance, the reduction of the transmitted wave energy is mainly associated with absorption. Indeed, although some fraction of the incident

light energy is reflected at the left-hand interface of the periodic stack in Fig. 2, this fraction remains limited even in the case of strong absorption, as seen in Fig. 8(b). So, the main source of the energy losses in a slow wave resonator is absorption, which is a natural side effect of the Faraday rotation enhancement (some important reservations can be found in [14]).

In the case of magnetic cavity resonance, the situation is fundamentally different. In this case, the energy losses associated with absorption cannot be much different from those of slow wave resonator, provided that both arrays display comparable enhancement of Faraday rotation. What is fundamentally different is the reflectivity. An inherent problem with any (localized) defect mode is that any significant absorption makes it inaccessible. Specifically, if the D-layer in Fig. 1 displays an appreciable absorption, the entire layered array becomes highly reflective. As a consequence, a major portion of the incident light energy is reflected from the stack surface and never even reaches the magnetic D-layer. Such a behavior is illustrated in Fig. 6, where we can see that as soon as the absorption coefficient γ exceeds certain value, further increase in γ leads to high reflectivity of the layered structure. In the process, the total absorption a reduces, as seen in Fig. 5, but the reason for this reduction is that the light simply cannot reach the magnetic layer. There is no Faraday rotation enhancement in this case.

Acknowledgments: Effort of A. Figotin and I. Vitebskiy is sponsored by the Air Force Office of Scientific Research, Air Force Materials Command, USAF, under grant number FA9550-04-1-0359.

[1] L. D. Landau, E. M. Lifshitz, L. P. Pitaevskii. *Electrodynamics of continuous media*. (Pergamon, N.Y. 1984).
[2] A. G. Gurevich and G. A. Melkov. *Magnetization Oscillations and Waves*. (CRC Press, N.Y. 1996).
[3] M. Inoue, et all. *Magnetophotonic crystals (Topical Review)*. J. Phys. D: Appl. Phys. 39, R151–R161 (2006).
[4] I. Lyubchanskii1, N. Dadoenkova1, M. Lyubchanskii1, E. Shapovalov, and T. Rasing. *Magnetic photonic crystals*. J. Phys. D: Appl. Phys. 36, R277–R287 (2003)
[5] M. Inoue, K. Arai, T. Fuji, and M. Abe. *One-dimensional magnetophotonic crystals*. J. Appl. Phys. 85, 5768 (1999).
[6] M. Levy and A. A. Jalali. *Band structure and Bloch states in birefringent onedimensional magnetophotonic crystals: an analytical approach*. J. Opt. Soc. Am. B, 24, 1603-1609 (2007).
[7] M. Levy and R. Li. *Polarization rotation enhancement and scattering mechanisms in waveguide magnetophotonic crystals*. Appl. Phys. Lett. 89, 121,113 (2006)..
[8] S. Khartsev and A. Grishin. *High performance magneto-optical photonic crystals*. J. Appl. Phys. 101, 053,906 (2007).
[9] S. Kahl and A. Grishin. *Enhanced Faraday rotation in all-garnet magneto-optical photonic crystal*. Appl. Phys. Lett. 84, 1438 (2004).
[10] S. Erokhin, A. Vinogradov, A. Granovsky, and M. Inoue. Field Distribution of a Light Wave near a Magnetic Defect in One-Dimensional Photonic Crystals. Physics of the Solid State, 49, 497 (2007).
[11] Vol. 49
[12] A. Figotin, and I. Vitebsky. *Nonreciprocal magnetic photonic crystals*. Phys. Rev. **E**63, 066609 (2001).
[13] A. Figotin, and I. Vitebskiy. *Electromagnetic unidirectionality in magnetic photonic crystals*. Phys. Rev. **B**67, 165210 (2003)
[14] A. Figotin and I. Vitebskiy. *Absorption suppression in photonic crystals*. Phys. Rev. **B**77, 104421 (2008)

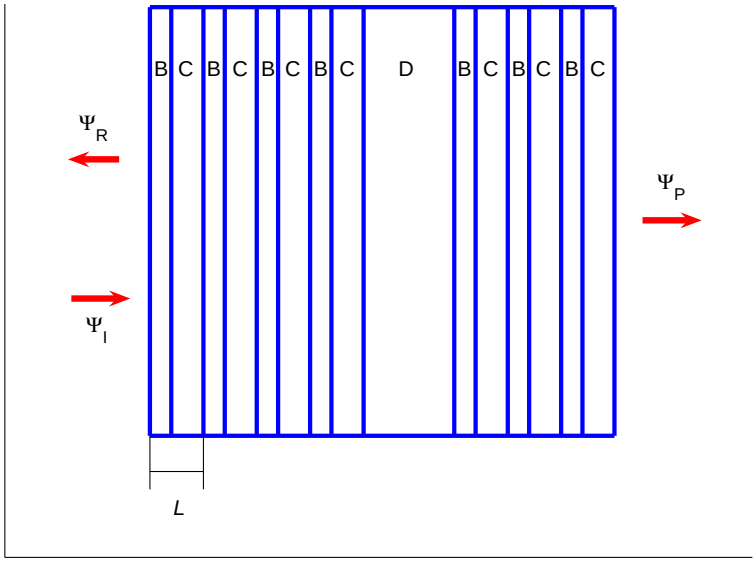

Figure 1. (Color online) Magnetic resonance cavity composed of magnetic layer D sandwiched between a pair of identical periodic non-magnetic stacks (Bragg reflectors). The incident wave Ψ_I is linearly polarized with $E \parallel x$. Due to the nonreciprocal circular birefringence of the magnetic material of D-layer, the reflected wave Ψ_R and the transmitted wave Ψ_P are both elliptically polarized.

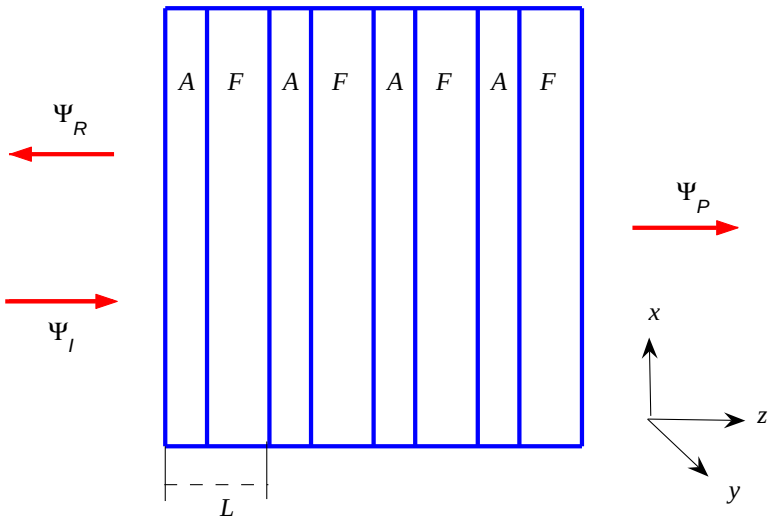

Figure 2. (Color online) Periodic layered structure composed of alternate magnetic (F) and dielectric (A) layers. The F-layers are made of the same lossy magnetic material as the D-layer in Fig. 1. L is the unit cell length. The incident wave Ψ_I is linearly polarized with $E \parallel x$. Due to the nonreciprocal circular birefringence of the magnetic material of the F-layers, the reflected wave Ψ_R and the transmitted wave Ψ_P are both elliptically polarized.

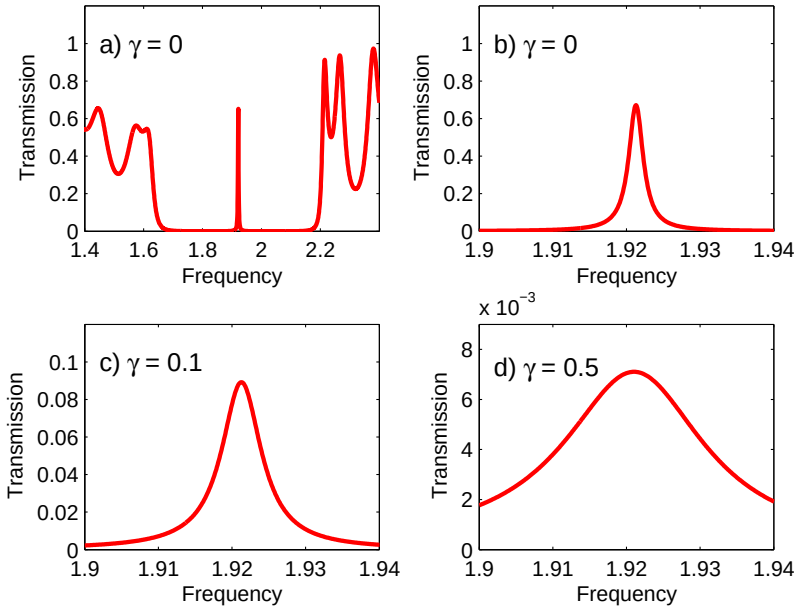

Figure 3. (Color online) Transmission dispersion of the layered array in Fig. 1 for different values of absorption coefficient γ of the D-layer. Circular birefringence α is negligible. Fig. (b) shows the enlarged portion of Fig. (a) covering the vicinity of microcavity resonance.

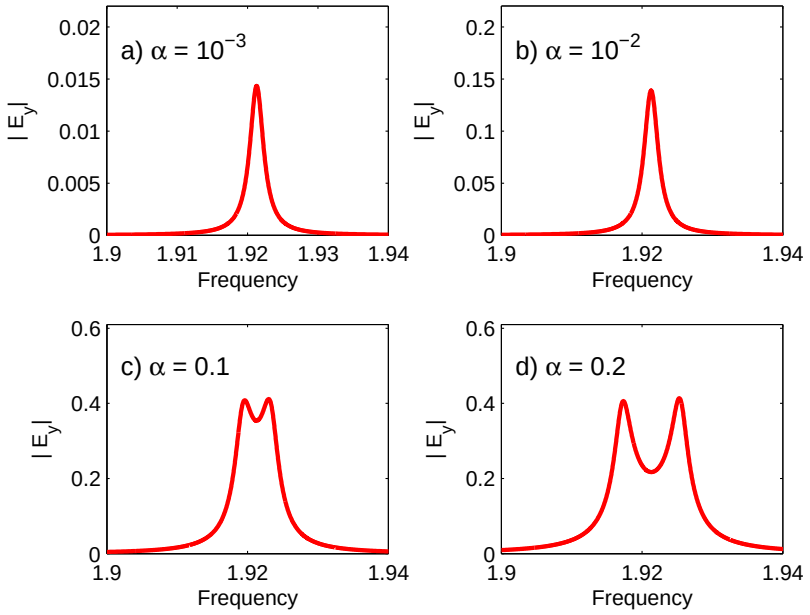

Figure 4. (Color online) Frequency dependence of polarization component $|E_y|$ of the wave transmitted through layered array in Fig. 1 for different values of circular birefringence α of the D-layer and zero absorption. When circular birefringence α is strong enough, the cavity resonance splits into a pair of twin resonances, corresponding to two circularly polarized modes with opposite sense of rotation. The incident wave is linearly polarized with $\vec{E} \parallel x$.

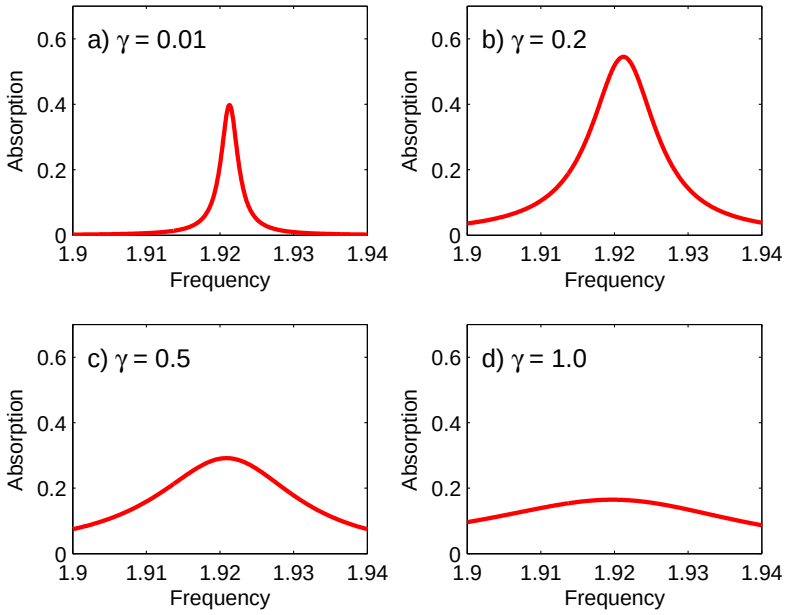

Figure 5. (Color online) Frequency dependence of absorption of the layered array in Fig. 1 for different values of absorption coefficient γ of the D-layer. Circular birefringence α is negligible. The frequency range shown covers the vicinity of microcavity resonance. Observe that the stack absorption decreases after coefficient γ exceeds certain value, which is in sharp contrast with the case of a periodic stack, shown in Figs. 8.

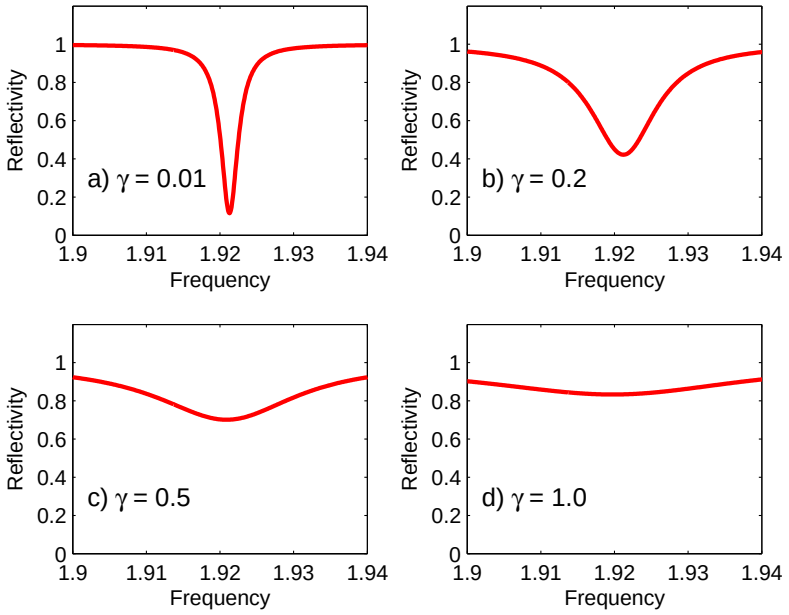

Figure 6. (Color online) Frequency dependence of the reflectance r of the layered array in Fig. 1 for different values of absorption coefficient γ of the D-layer. Circular birefringence α is negligible. The frequency range shown covers the vicinity of microcavity resonance. Observe that if the absorption coefficient γ of D-layer increases, the stack reflectivity also increases approaching unity. Such a behaivior is line with frequency dependence of the stack absorption shown in Fig. 5. It is in sharp contrast with the case of a periodic stack, shown in Figs. 8.

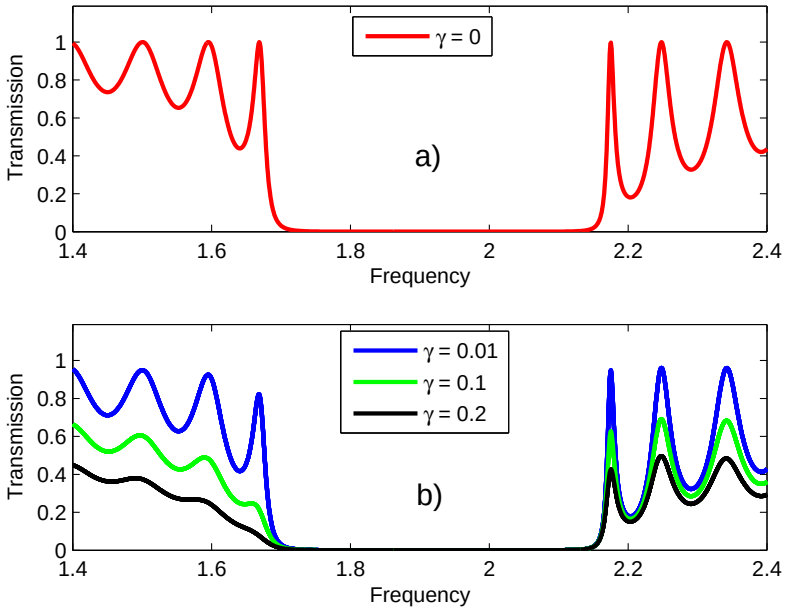

Figure 7. (Color online) Transmission dispersion of periodic layered structure in Fig. 2 for different values of absorption coefficient γ of the F-layers. Circular birefringence α is negligible.

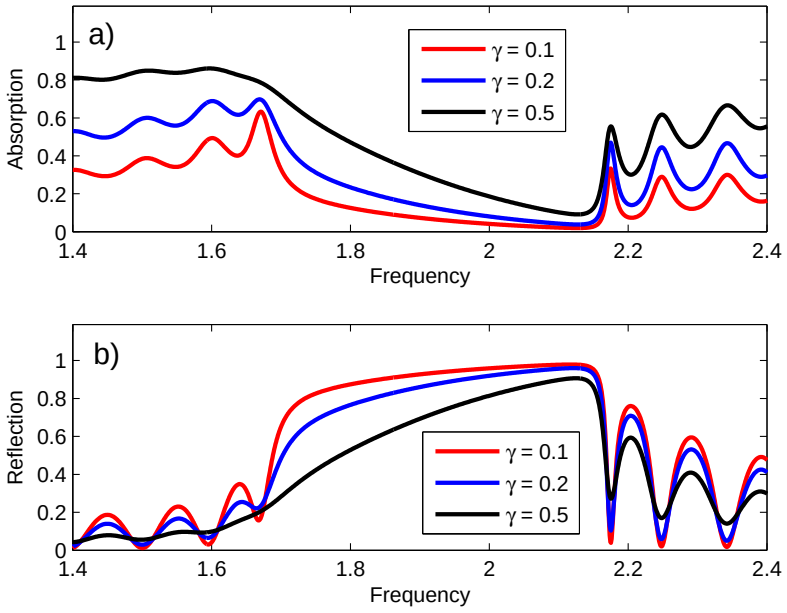

Figure 8. (Color online) Frequency dependence of (a) absorption and (b) transmission of periodic layered structure in Fig. 2 for different values of absorption coefficient γ of the F-layers. Circular birefringence α is negligible.

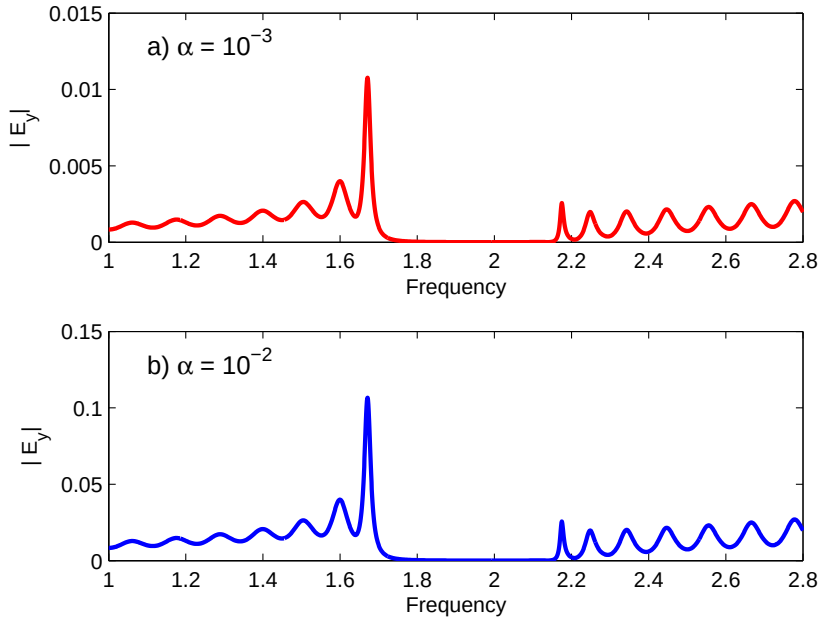

Figure 9. (Color online) Frequency dependence of polarization component $|E_y|$ of the wave transmitted through the periodic layered structure in Fig. 2 for different values of circular birefringence α of the F-layers and zero absorption. The incident wave is linearly polarized with $\vec{E} \parallel x$.

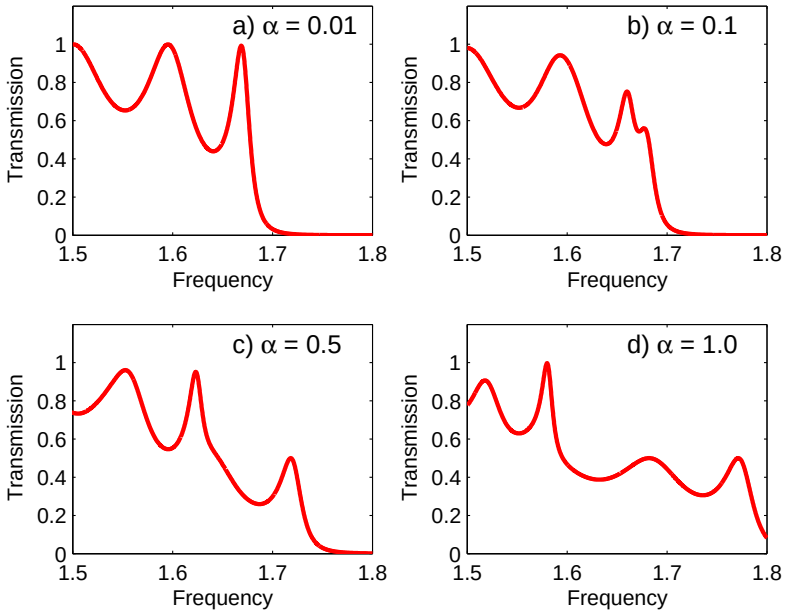

Figure 10. (Color online) Transmission dispersion of periodic layered structure in Fig. 2 for different values of circular birefringence α of the F-layers and zero absorption. When circular birefringence α is large enough, each transmission resonance splits into a pair of twin resonances, corresponding to two circularly polarized modes with opposite sense of rotation. The incident wave polarization is linear.

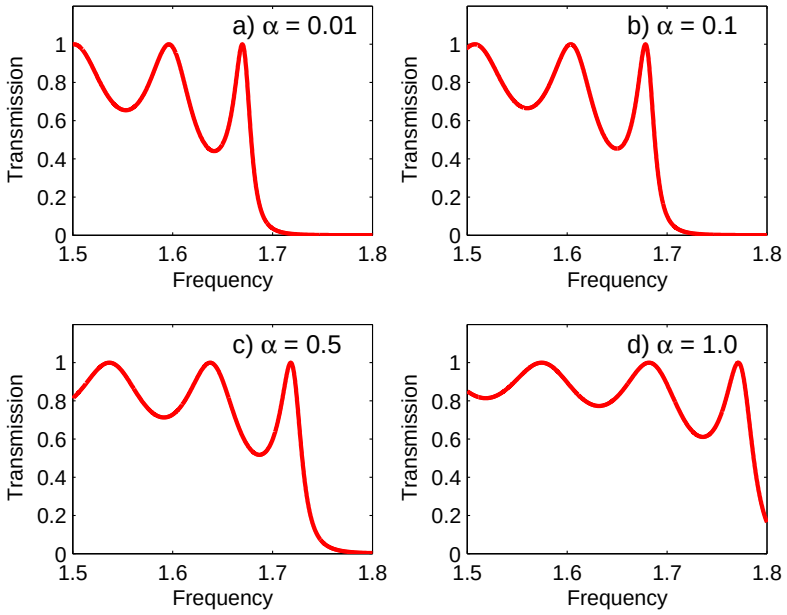

Figure 11. (Color online) The same as in Fig. 10, but the incident wave polarization is circular with positive sense of rotation.

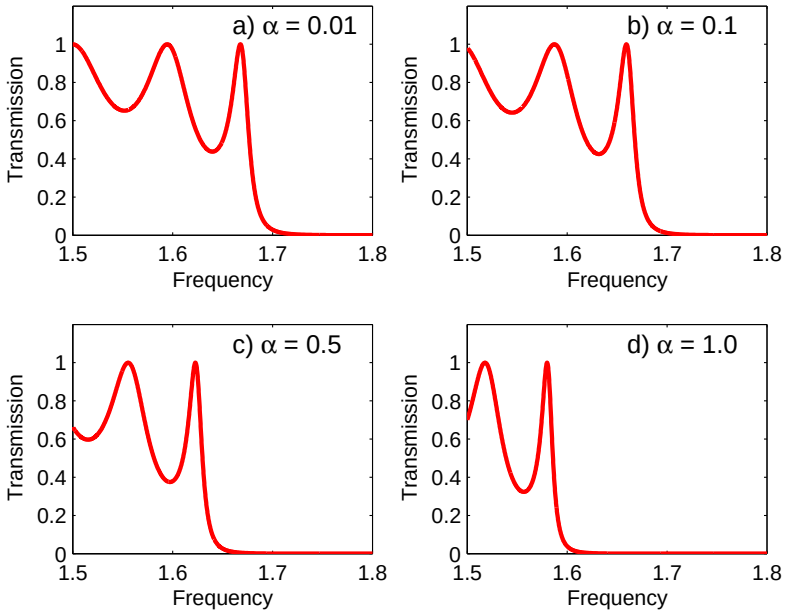

Figure 12. (Color online) The same as in Figs. 10 and 11, but the incident wave polarization is circular with negative sense of rotation.